Immunohistochemical Detection and Molecular Characterization of *IDH*-mutant Sinonasal Undifferentiated Carcinomas

Jeffrey K. Mito, MD, PhD, Justin A. Bishop, MD,† Peter M. Sadow, MD, PhD,‡ Edward B. Stelow, MD,§ William C. Faquin, MD, PhD,‡ Stacey E. Mills, MD,§ Jeffrey F. Krane, MD, PhD,* Christopher A. French, MD,* Christopher D.M. Fletcher, MD, FRCPath,* Jason L. Hornick, MD, PhD,* Lynette M. Sholl, MD,*|| and Vickie Y. Jo, MD**

Abstract: Recent studies have identified recurrent isocitrate dehydrogenase 2 (*IDH2*) mutations in a subset of sinonasal undifferentiated carcinomas (SNUCs); however, the true frequency of *IDH* mutations in SNUC is unknown. We evaluated the utility of mutation-specific IDH1/2 immunohistochemistry (IHC) in a large multi-institutional cohort of SNUC and morphologic mimics. IHC using a multispecific antibody for IDH1/2 (R132/R172) mutant protein was performed on 193 sinonasal tumors including: 53 SNUCs, 8 poorly differentiated carcinomas (PDCARs) and 132 histologic mimics. Mutant IDH1/2 IHC was positive in 26/53 SNUCs (49%; 20 strongly positive and 6 weak) and 3/8 PDCARs (37.5%; 2 strong; 1 weak) but was absent in all other tumor types (0/132). Targeted next-generation sequencing (NGS) on a subset of SNUC/PDCAR (6 strong and 3 weak positive for IDH1/2 IHC; 7 negative) showed frequent *IDH2* R172X mutations (10/16) and a single *IDH1* R132C mutation. All 6 cases with strong positive mutant IDH1/2 staining and NGS had *IDH2* R172S/G mutations. The 3 IHC-weak cases all had *IDH2* R172T mutations. Among the 7 tested cases that were negative for mutant IDH1/2 IHC, NGS detected 1 case each with *IDH2* R172T and *IDH1* R132C mutation. *IDH*-mutant carcinomas also had frequent mutations in *TP53* (55%) and activating mutations in *KIT* (45%) or the PI3K pathway (36%). Mutation-specific IDH1/2 IHC identifies *IDH* mutations in SNUC, however, it lacks sensitivity for the full range of *IDH* mutations. These findings suggest that *IDH*-mutant sinonasal carcinoma may represent a distinct pathobiological entity with therapeutic implications that can be identified by a combined approach of multispecific IDH1/2 IHC and sequencing.

Key Words: sinonasal undifferentiated carcinoma, IDH1, IDH2, SNUC, sinonasal carcinoma

(*Am J Surg Pathol* 2018;42:1067–1075)

From the *Department of Pathology; ||Center for Advanced Molecular Diagnostics, Brigham and Women's Hospital and Harvard Medical School; ‡Department of Pathology, Massachusetts General Hospital and Harvard Medical School, Boston, MA; †Department of Pathology, University of Texas Southwestern Medical Center, Dallas, TX; and §Department of Pathology, University of Virginia, Charlottesville, VA.

Conflicts of Interest and Source of Funding: The authors have disclosed that they have no significant relationships with, or financial interest in, any commercial companies pertaining to this article.

Correspondence: Vickie Y. Jo, MD, Department of Pathology, Brigham and Women's Hospital, 75 Francis Street, Boston, MA 02115 (e-mail: vjo@partners.org).

Supplemental Digital Content is available for this article. Direct URL citations appear in the printed text and are provided in the HTML and PDF versions of this article on the journal's website, www.ajsp.com.

Sinonasal undifferentiated carcinoma (SNUC) is a rare tumor that accounts for 3% to 5% of all sinonasal carcinomas.[1] First described in 1986 by Frierson et al,[2] patients with SNUC typically present with large, locally aggressive tumors with frequent involvement of the orbit and skull base.[3] Outcomes for affected patients are poor with a median survival of ∼22 months, even in the face of multimodality therapy.[4] Morphologically, SNUC consists of undifferentiated-appearing tumor cells with large round-to-ovoid nuclei with frequent prominent nucleoli and varying amounts of cytoplasm arranged in sheets, lobules, or trabeculae, and shows a nonspecific immunophenotype that includes expression of broad spectrum keratins, variable positivity for p63 (but not p40) and limited expression of neuroendocrine markers.[5,6]

SNUC is considered a diagnosis of exclusion, and has historically represented a heterogenous group of tumors. Since its original description, numerous distinct clinicopathologic entities and molecularly defined subsets have been identified in the sinonasal tract, which include NUT carcinoma,[7,8] Human papillomavirus (HPV)-related carcinomas of the sinonasal tract (including HPV-related multiphenotypic sinonasal carcinoma),[9,10] SMARCB1-deficient sinonasal carcinoma,[11,12] and SMARCA4-deficient sinonasal carcinoma.[13,14] Recently, recurrent mutations in isocitrate dehydrogenase 2 (*IDH2*) at the known hotspot R172 have been identified in a subset of SNUC.[14,15] Our group also reported 3 cases of SNUC with *IDH2* R172 mutations (R172S or R172M) that showed immunohistochemical (IHC) reactivity for a multispecific antibody for mutant IDH1/2 (mIDH1/2), which may prove to be a useful diagnostic marker.[14] Notably, the identification of *IDH* mutations also has significant therapeutic implications, as mutant IDH inhibitors have shown promise in the

treatment of other malignancies with *IDH* mutations, such as acute myeloid leukemia (AML)[16] and glioma.[17]

In this study, we evaluate the extent of IHC expression of mIDH1/2 in a large multi-institutional cohort of 53 SNUCs, and assess the diagnostic utility of mIDH1/2 IHC using a diverse group of morphologic mimics in the sinonasal tract. We also analyze a subset of SNUCs with targeted next-generation sequencing (NGS) to further characterize the genetic features of this rare and poorly understood sinonasal malignancy.

MATERIALS AND METHODS

This study was performed with approval of the Brigham and Women's Hospital Institutional Review Board. Cases diagnosed as SNUC (n = 53) were identified from the authors' surgical pathology and consult files. All diagnoses of SNUC were rendered or confirmed by specialists in head and neck pathology at their respective institutions (J.A.B., P.M.S., E.B.S., W.C.F., S.E.M., J.F.K., C.A.F., V.Y.J.), and all histologic mimics were excluded (e.g., NUT carcinoma, SMARCB1-deficient carcinoma, and nasopharyngeal carcinoma). Hematoxylin and eosin–stained slides were centrally reviewed (J.K.M. and V.Y.J.). One hundred forty additional sinonasal malignancies were identified in the Brigham and Women's Hospital archives (Table 1), including 8 cases originally classified as poorly differentiated carcinoma (PDCAR) based on the presence of focal morphologic or IHC features suggestive of squamous (3/8), glandular (1/8), or neuroendocrine (4/8) differentiation that did not fit into any specific World Health Organization category.

For the 193 cases, IHC was performed on 4 μm thick formalin-fixed paraffin-embedded whole tissue sections after deparaffinization at 42°C. Antigen retrieval was performed utilizing Target Retrieval Solution (Dako, Carpinteria, CA) in a pressure cooker. Slides were incubated with a multispecific antibody against mIDH1/2 (clone MsMab-1, 1:100; Millipore Sigma, Darmstadt, Germany) followed by the Novolink detection system (Leica, Buffalo Grove, IL). As a positive control, a colorectal adenocarcinoma with a known *IDH2* R172S mutation was stained in parallel. mIDH1/2 IHC was scored (J.K.M. and V.Y.J.) blinded to diagnosis. Cases were considered positive when granular cytoplasmic staining was present in > 10% of tumor cells, and staining intensity was recorded as strong or weak. SMARCA4 IHC was performed using a monoclonal antibody against BRG-1 (clone EPR3912, 1:50; Abcam, Cambridge, MA) after antigen retrieval as described above.

NGS was performed utilizing the OncoPanel assay,[18] which consists of targeted exonic sequencing of 447 cancer-related genes, and 191 intronic regions across 60 genes for detection of gene rearrangements (Supplemental Table 1, Supplemental Digital Content 1, http://links.lww.com/PAS/A612). DNA was extracted from formalin-fixed paraffin-embedded tissue using the QIAamp DNA mini kit (Qiagen, Valencia, CA) per manufacturer's instructions and sonicated to target fragment length of 270 bp. Hybrid-capture libraries for sequencing were constructed as previously described and samples sequenced on the Illumina HiSeq. 2500, per manufacturer's instructions (Illumina, San Diego, CA).[19] Sequence analysis was performed as previously described.[14] All detected alterations, including single nucleotide variants, copy number alterations, and translocation calls, were manually reviewed and annotated (L.M.S.).

TABLE 1. IHC Expression of Mutant IDH1/2 in 193 Sinonasal Malignancies

		n (%)		
Tumor Types	**Total Cases**	**mIDH1/2 Negative**	**mIDH1/2 Weak Positive**	**mIDH1/2 Strong Positive**
SNUC	53	27 (51)	6 (11)	20 (38)
PDCAR*	8	5 (63)	1 (13)	2 (25)
Basaloid carcinoma, NOS*	6	6 (100)	0	0
Adenoid cystic carcinoma	10	10 (100)	0	0
Alveolar rhabdomyosarcoma	13	13 (100)	0	0
Ewing sarcoma	1	1 (100)	0	0
Extranodal NK/T-cell lymphoma	4	4 (100)	0	0
HPV-related multiphenotypical sinonasal carcinoma	3	3 (100)	0	0
SMARCB1-deficient sinonasal carcinoma	5	5 (100)	0	0
Intestinal-type adenocarcinoma	6	6 (100)	0	0
Malignant melanoma	14	14 (100)	0	0
Neuroendocrine carcinoma	8	8 (100)	0	0
Nasopharyngeal carcinoma	14	14 (100)	0	0
Non-intestinal adenocarcinoma	3	3 (100)	0	0
NUT carcinoma	10	10 (100)	0	0
Olfactory neuroblastoma	12	12 (100)	0	0
Squamous cell carcinoma, Human papillomavirus-associated	6	6 (100)	0	0
Squamous cell carcinoma	17	17 (100)	0	0

*These diagnoses were descriptive and based on morphologic and IHC features, which were not sufficiently diagnostic to be categorized per the WHO classification.

RESULTS

Clinical Features of SNUC Study Cohort

Fifty-three cases of SNUC included 40 men and 13 women, overall age ranged from 19 to 82 years (median, 58 y). On the basis of available data (38/53 cases), 22 cases involved multiple anatomic sites, typically the nasal cavity (16) and associated sinuses including the ethmoid (15), maxillary (8), sphenoid (8), and/or frontal (5) sinuses. Many cases involving multiple anatomic sites also showed intracranial extension (7) or involvement of the orbit (6) and/or skull base (5). Of the remaining cases, there were more limited clinical data, and these tumors were sampled from the nasal cavity (10), maxillary (4), ethmoid (2), and sphenoid sinuses (1).

mIDH1/2 IHC

Overall, 26 of 53 of SNUCs (49%) showed mIDH1/2 positivity. Twenty cases (38%) showed diffuse strong granular cytoplasmic staining for mIDH1/2 (Figs. 1A-F). In addition, weak granular cytoplasmic mIDH1/2 staining was observed in 6 SNUCs (11%) (Fig. 2). Among PDCARs, strong mIDH1/2 positivity was present in 2/8 (25%) of cases (Figs. 1H-I) and 1 case (12.5%) showed weak positive staining. The remaining SNUCs (27/53) and PDCARs (5/8) were completely negative by mIDH1/2 IHC (Fig. 3). No other histologic mimics in the study cohort showed mIDH1/2 staining, including: NUT carcinoma (0/10), SMARCB1-deficient sinonasal carcinoma (0/5), HPV-related multiphenotypic sinonasal carcinoma (0/3), nasopharyngeal carcinoma (0/14), olfactory neuroblastoma (0/12), and high-grade neuroendocrine carcinoma (0/8). The results of mIDH1/2 IHC for the cohort are summarized in Table 1.

NGS Results

Targeted NGS was performed on 20 sinonasal carcinomas including 18 SNUCs and 2 PDCARs. Fourteen SNUC cases and 2 PDCARs were successfully subjected to targeted NGS, including cases with positive (n = 6), weak (n = 3), and

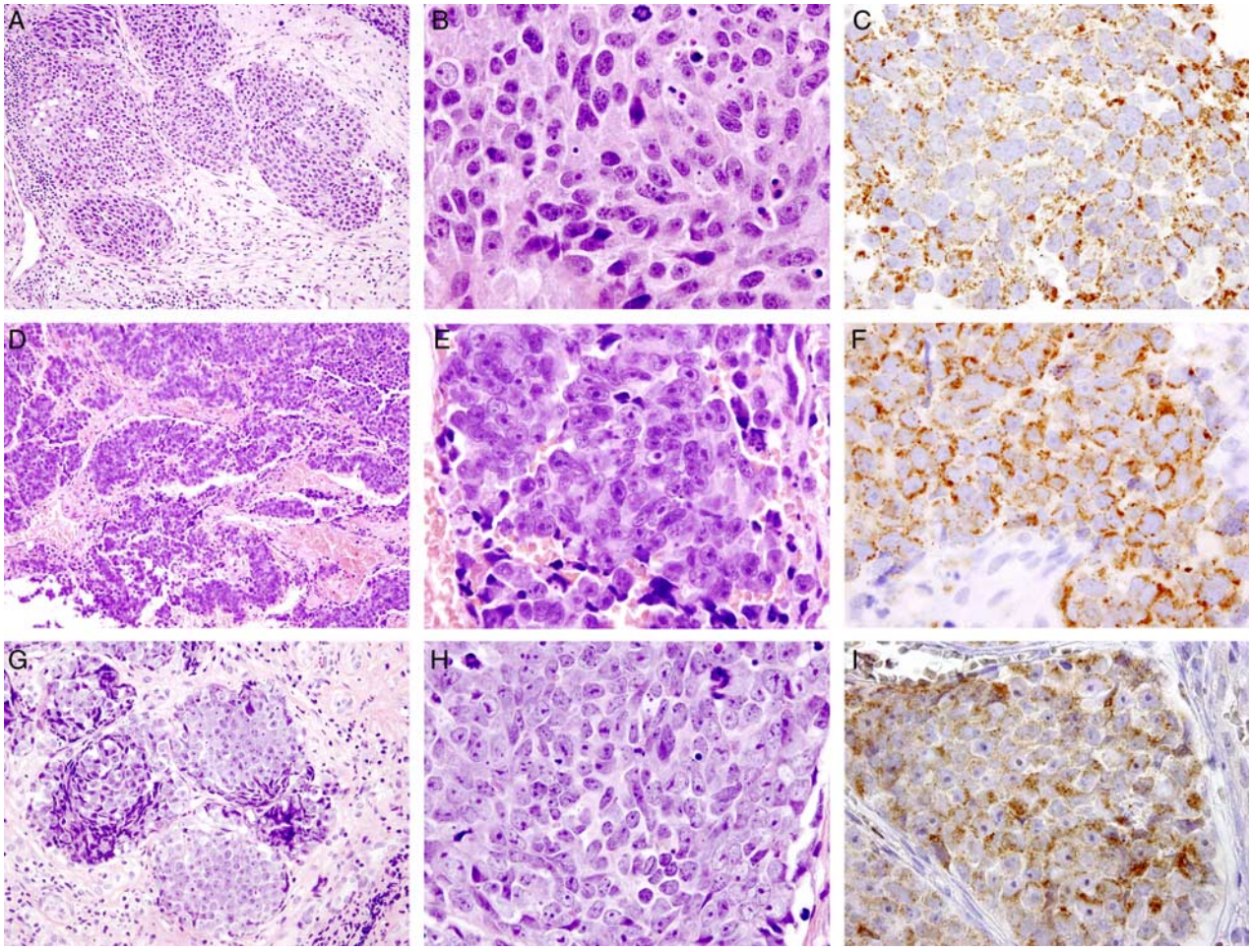

FIGURE 1. SNUCs showed frequent strong expression (38%) of mutant IDH1/2 R132/R172 (mIDH1/2). Cases of SNUC with sequence-verified *IDH2* R172S mutations and mIDH1/2 expression showed a frequent nested growth pattern at low power (A and D, hematoxylin and eosin [H&E]) with prominent nucleoli (B and E, H&E). IHC for mutant IDH1/2 showed strong granular cytoplasmic staining (C and F). A subset of cases previously classified as PDCAR (25%), including a case with an *IDH2* R172S mutation, showed strong positive mIDH1/2 IHC (25%). mIDH1/2-positive PDCARs had similar morphologic features including a nested growth pattern (G, H&E) with frequent prominent nucleoli (H, H&E) and strong granular cytoplasmic mIDH1/2 staining (I).

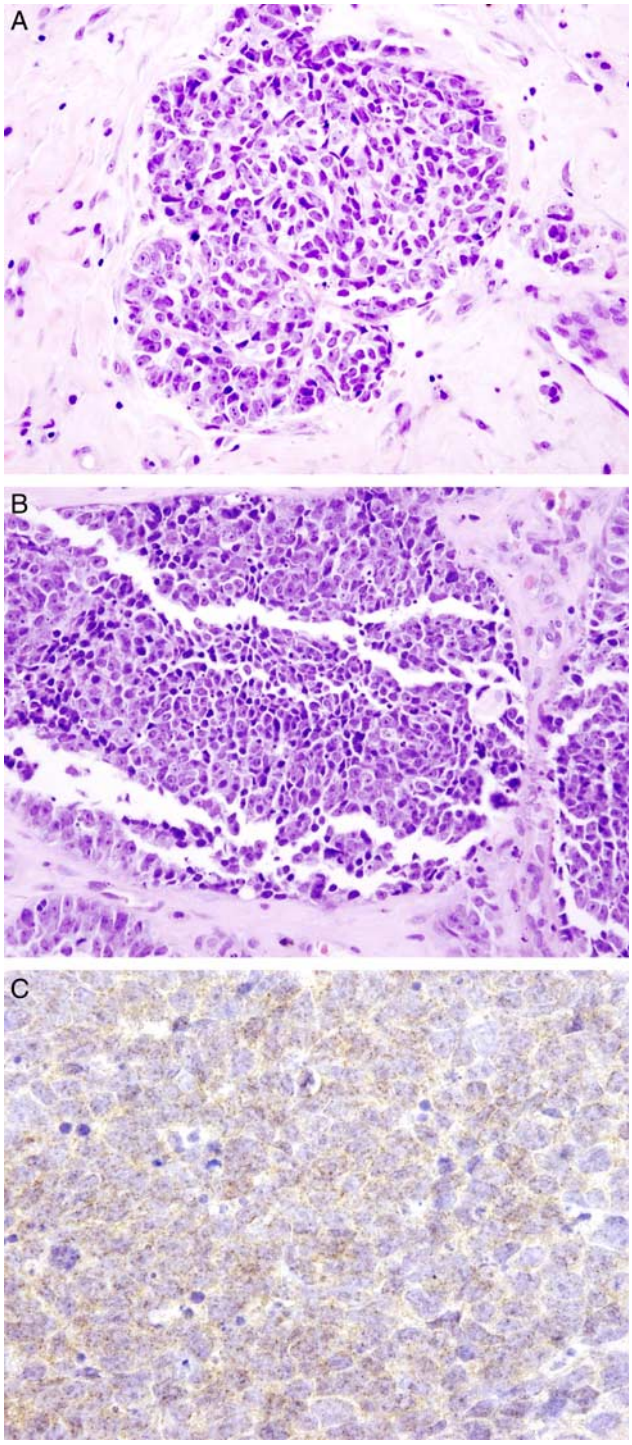

FIGURE 2. A subset of SNUC (6 cases) and 1 poorly differentiated sinonasal carcinoma that also showed a predominant nested growth pattern (A and B, H&E), showed weak granular cytoplasmic mIDH1/2 staining (C); 3 of these SNUCs were sequenced and confirmed to have *IDH2* R172T mutations.

negative (n = 7) mIDH1/2 IHC staining. Cases negative by mIDH1/2 IHC were selected for sequencing based on shared morphologic features (see below) with mIDH1/2 IHC positive cases. The median sequence coverage was 150 (range, 24 to 389) with a median percentage of sequences achieving > 30-fold coverage of 97% (range, 29% to 99%). The key pathogenic variants detected by NGS are summarized in Figure 4 (Supplemental Table 2, Supplemental Digital Content 2, http://links.lww.com/PAS/A613 for a complete list of single nucleotide variants and selected copy number variants). Four SNUCs failed NGS due to low sequencing quality metrics.

Overall, *IDH* mutations were detected in 11 of 16 SNUC/PDCARs. Ten SNUCs/PDCARs had *IDH2* mutations. All *IDH2* mutations involved codon R172, comprised of R172S (4/10, including both mIDH1/2 IHC positive PDCARs), R172T (4/10), and R172G (2/10) mutations. No *IDH2* codon R140 mutations were identified. All cases with R172S and R172G mutations had strong positive mIDH1/2 IHC. Of the 4 cases with *IDH2* R172T mutations, 3 of 4 cases showed diffuse weak granular staining (Fig. 2), whereas 1 case was negative by mIDH1/2 IHC. Finally, an *IDH1* R132C mutation was identified in the 11th case, which also had relative loss of the wild-type *IDH1* allele by copy number analysis. This case was negative for mIDH1/2 IHC.

Among *IDH*-mutant sinonasal carcinomas, frequent co-occurrence of *TP53* mutations (6/11), *KIT* mutations (5/11), and activating PI3K pathway mutations (4/11) were also identified. The *KIT* mutations included *KIT* S476C located in exon 9 in a patient with a focal amplification involving the *KIT* gene. Although not a canonical pathogenic mutation, the fact that the S476C variant has been previously reported in another KIT-driven tumor type,[20] combined with the presence of focal amplification, suggests that this mutation may be functionally activating. Additional *KIT* mutations identified included 2 activating in-frame deletions involving codons 578 to 579 and 419, an A829P mutation, and canonical activating D816V mutation. Activating PI3K pathway mutations included 1 case showing homozygous deletion of *PTEN*, 1 case with an *MTOR* F1888L activating mutation, and 2 cases with activating *PIK3CA* mutations (Q546R and E545K).

Among the 5 *IDH* wild-type tumors, 1 SMARCA4-deficient sinonasal carcinoma was identified, which showed biallelic inactivation including both a nonsense (c.4471C > T [p.R1491*]) and a frameshift mutation (c.3224_3225delTG [p.Y1076Pfs*5]) (Fig. 4). Subsequent IHC for SMARCA4 showed complete loss of expression in tumor cells (Fig. 5). In order to exclude the possibility of additional unidentified cases of SMARCA4-deficient sinonasal carcinoma in our cohort, we performed SMARCA4 IHC on all cases originally classified as SNUC or PDCAR with available material that were not subjected to NGS or that had other known molecular alterations (i.e., *IDH1/2* mutation) (n = 29). No additional cases showed loss of SMARCA4 expression; including SNUCs that underwent NGS (n = 16), the overall rate of SMARCA4 loss was 1 in 45 cases (2.2%).

Of the remaining 4 *IDH* wild-type SNUCs that underwent NGS, inactivation of *TP53* was identified in 3 tumors: 1 case with a frameshift mutation (c.111_123delCCAAGCAATGGAT [p.Q38Ifs*2]) and 430 bp deletion in the 5'-UTR, 1 case with a C135F missense mutation, and 1 case with a Y163* nonsense mutation. In the case with a *TP53*

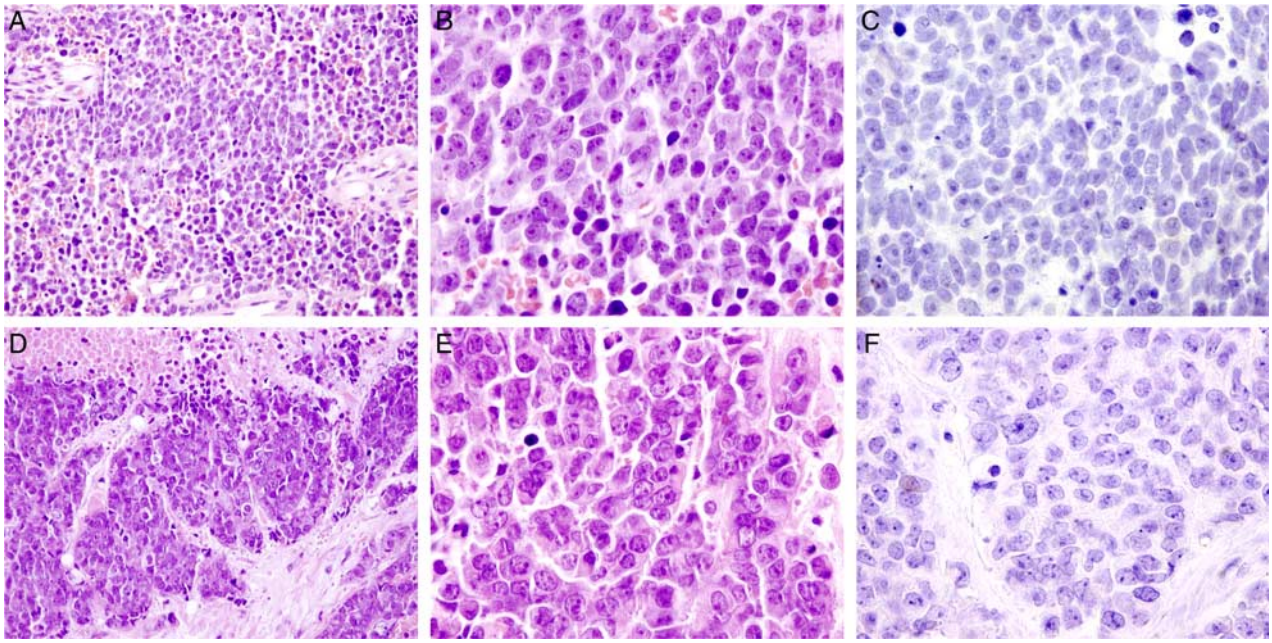

FIGURE 3. The majority of SNUC and poorly differentiated sinonasal carcinomas were completely negative for mIDH1/2 IHC, including all cases of SNUC with known wild-type *IDH1/2* status (A–C and D–F).

frameshift mutation and 5'-UTR deletion, concomitant inactivation of *RB1* and loss of *CDKN2A* was also identified.

Clinical and Morphologic Features of *IDH*-Mutant SNUC

Clinically, patients with *IDH*-mutant sinonasal carcinomas included 18 men and 7 women (M:F = 2.6:1) who presented over a wide age range (22 to 81 y; median, 62 y). Of the patients with available information regarding anatomic site (22/25), 15 of 22 presented with sinonasal masses involving multiple anatomic sites, typically the nasal cavity (13) and adjacent sinuses including the ethmoid (13), maxillary (7), sphenoid (6), and/or frontal (5) sinus with frequent intracranial (5), intraorbital (5), and/or skull base (4) involvement. Of the remaining 7 patients, more limited clinical information was available, 5 had disease involving

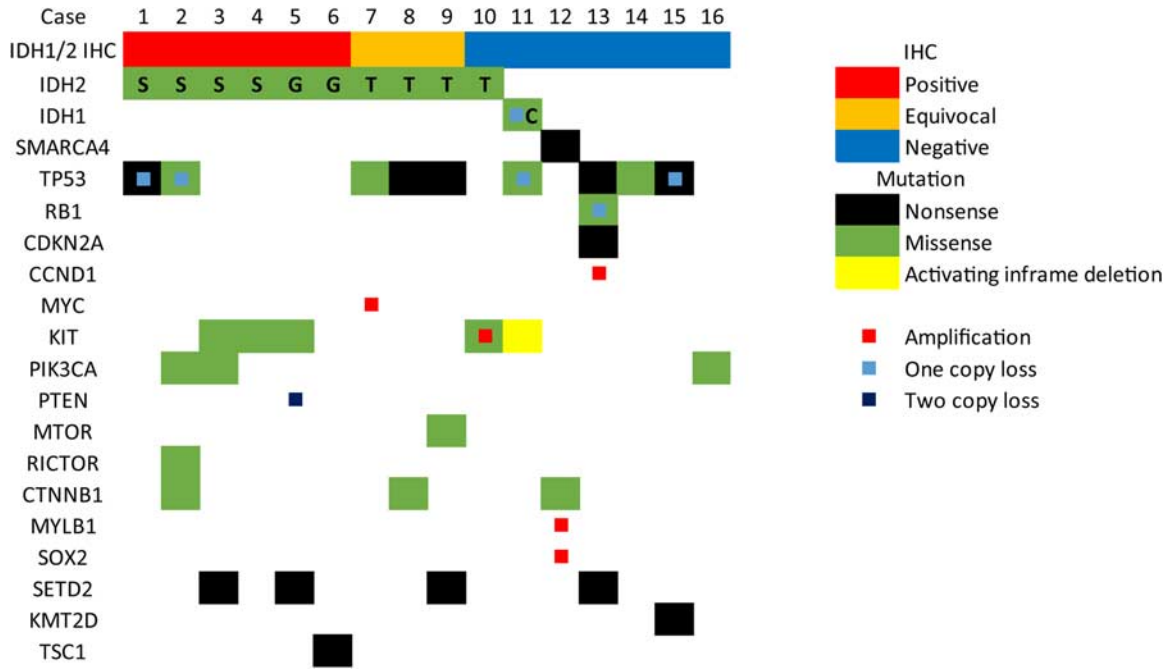

FIGURE 4. Summary of NGS results and associated mIDH1/2 IHC results.

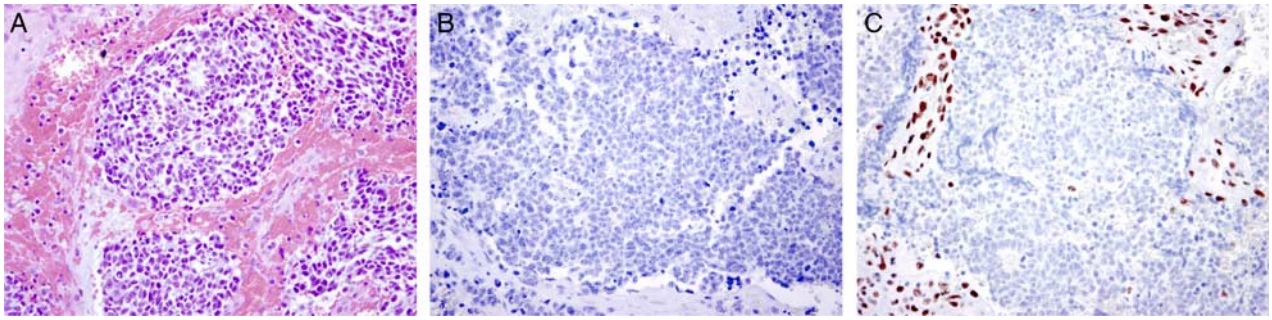

FIGURE 5. SMARCA4-difficient sinonasal carcinoma. A single case of SMARCA4-difficient sinonasal carcinoma was identified within the SNUC cohort, which showed similar morphologic features to cases of *IDH*-mutant SNUC (A, H&E), that was negative for mIDH1/2 by IHC (B) and showed complete loss of BRG-1 expression (*SMARCA4* gene product) by IHC (C).

the nasal cavity, and 1 each with tumor located in the skull base and the maxillary sinus.

Morphologically, most *IDH*-mutant sinonasal carcinomas (originally classified as SNUC or PDCAR) showed nested (19/25) or sheet-like (5/25) growth patterns and consisted of uniform but atypical moderate-to-large tumor cells with rounded to slightly elongated nuclei with frequently prominent nucleoli (16/25) and variable amounts of cytoplasm. Necrosis was frequent (16/25), and tumors showed high mitotic rates among cases with

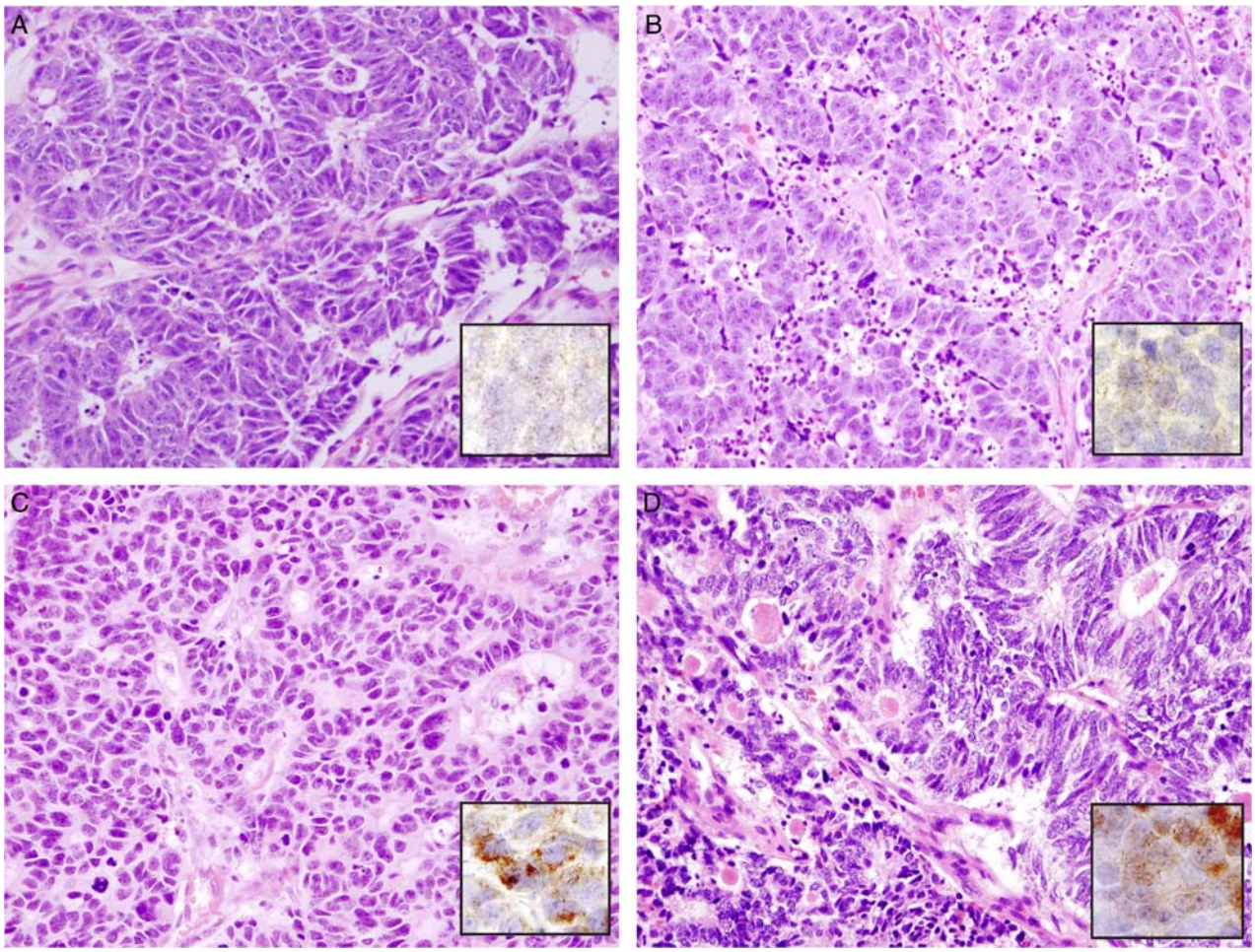

FIGURE 6. Infrequent morphologic features of *IDH*-mutant SNUCs. A subset of *IDH2* R172T-mutant SNUC showed foci with (A and B) trabecular growth (inset, mIDH1/2 IHC). Additional cases that were positive for mIDH1/2 IHC, but were not sequence verified showed (C and D) areas more reminiscent of glandular/tubular growth (inset, mIDH1/2 IHC).

sufficient material to evaluate (median, 37/10 high-power fields; field size, 0.25 mm^2; range, 10 to 69). Occasional cases showed foci with trabecular (2/25) or pseudoglandular/tubular (2/25) growth (Fig. 6). While the nested growth pattern and morphology were consistent features, these were not unique to cases with mIDH1/2 positivity and could not be used to distinguish from mIDH1/2 IHC negative cases of SNUC/PDCAR.

DISCUSSION

SNUC represents an aggressive disease that frequently involves multiple anatomic sites and is associated with poor survival. As demonstrated here and in prior studies, recurrent *IDH2* R172X mutations characterize a subset of SNUCs;[14,15] we also previously reported 3 *IDH*-mutant SNUCs to be immunoreactive for mIDH1/2 IHC (2 cases with R172S and 1 with R172M). Using the multispecific antibody MsMab-1 to screen a cohort of SNUC, PDCARs, and histologic mimics, we found that approximately one third of cases of SNUC/PDCAR (22/61) show strong mIDH1/2 expression by IHC. An additional 11% of cases (7/61) showed weak staining, which may be mistaken as equivocal or background staining. NGS performed on a subset of SNUCs demonstrated that positive mIDH1/2 staining correlated with mutant *IDH2* R172 status in all tumor samples submitted for NGS. In addition, we identified *IDH2* R172T mutations in 3 cases that showed weak mIDH1/2 staining. This suggests that mIDH1/2 staining of any intensity is predictive of *IDH1/2* mutational status and that the rate of *IDH1/2* mutations within morphologic SNUC/PDCAR cases within our cohort would be at least 48% (29/61).

IHC for mIDH1/2 is not entirely sensitive for the presence of *IDH* mutations. Among SNUCs that were negative by mIDH1/2 IHC, single cases with *IDH2* R172T and *IDH1* R132C mutations were identified. Previous studies utilizing the multispecific antibody MsMab-1 have shown that it recognizes multiple pathogenic IDH1[21] and IDH2 mutations.[22] However, it is not unexpected that mIDH1/2 IHC did not detect all cases with *IDH* mutations as previous reports and ELISA studies have shown that not all IDH1/2 mutations can be detected by MsMab-1.[21,22] Mutations previously shown to be detectable by MsMab-1 include: *IDH2* R172G, R172M, R172S, and *IDH1* R132S, R132G R132H mutations. A subset of *IDH1* (including R132C, R132V, R132P, R132I, and R132L) and *IDH2* (including R172K, R172T, and R172W) mutations; however, are not detected by the antibody.[21,22] These prior reports are consistent with our observation that SNUCs with *IDH2* R172T showed either weak positive or negative mIDH1/2 staining. Given that not all *IDH1/2* mutations are detected by MsMab-1, the addition of other complimentary antibodies that detect distinct *IDH* mutations may enhance the overall utility of IHC in identifying *IDH*-mutant SNUCs, though molecular confirmation may be necessary for some cases.

IDH-mutant SNUC frequently showed a nested growth pattern of uniform epithelioid cells with large nuclei and prominent nucleoli. However, these morphologic features are not specific for *IDH*-mutant tumors, and overlap with many other sinonasal malignancies including SMARCB1-deficient sinonasal carcinoma[11,12] and NUT carcinoma,[8] among others. Importantly, no histologic mimics of SNUC had any degree of mIDH1/2 staining, consistent with previous reports that that *IDH* mutations are highly specific for SNUC among head and neck malignancies.[14]

Within our SNUC cohort, we detected *IDH2* R172S, R172G, and R172T mutations, similar to prior studies, as well as an *IDH1* R132C mutation. We also identified concomitant *KIT* mutations (45%) and/or PI3K pathway mutations (36%). Dogan et al[15] identified 2 concurrent *KIT* mutations among 12 *IDH2* R172X mutant sinonasal carcinomas (17%); a similar rate of PI3K pathway activating mutations was also observed in their study (2/12, 17%). In contrast, prior work from our group did not identify concurrent *KIT* mutations among 6 *IDH2* mutant SNUC, but did detect PI3K pathway activating mutations among 2 of 6 cases (33%).[14] In this multi-institutional study, we identified higher rates of activating *KIT* mutations among *IDH*-mutant sinonasal carcinoma (5/11, 45%) and a similar rate of PI3K pathway activating mutations as previous studies (4/11, 36%). The prevalence of these mutations among *IDH*-mutant SNUCs is currently unknown, but may be better understood as additional cases are identified and the use of NGS in routine clinical care expands. A recent study by Ali et al[23] reported *IDH2* R172 mutations in 17 cases of nasopharyngeal carcinoma, however these cases were not annotated on clinical, radiologic, or pathologic bases and EBV status for the *IDH*-mutant cases was not specifically provided. Given the ambiguous pathologic classification of their cohort,[24] it is highly likely that many of these cases reported by Ali and colleagues represent sinonasal primary tumors given the lack of evidence of *IDH1/2* hotspot mutations in nasopharyngeal carcinoma in our experience and in the published literature,[25–27] where no mutation in the known hotspots in *IDH2* R140 and R172 have been identified.

We identified 1 case with SMARCA4 biallelic inactivation by NGS; 2 cases of SMARCA4-deficient sinonasal carcinomas have recently been reported.[13,14] This case showed overlapping morphologic features with other SNUCs in this cohort, including a nested growth pattern with occasional pseudorosette structures, scattered nucleoli, and a high mitotic rate (25 mitoses/10 high-power fields). While mIDH1/2 IHC was negative in this present case, the morphologic features prompted selection for NGS analysis. In addition to biallelic *SMARCA4* inactivation, NGS also identified an activating mutation in *CTNNB1*, which encodes β-catenin. The SMARCA4-deficient sinonasal carcinoma previously reported by our group (identified in a separately studied cohort of SNUCs) had a concomitant inactivating mutation in *APC*.[14] Both *CTNNB1* and *APC* are part of the canonical WNT signaling pathway. Recurrent *SMARCA4* mutations have been identified in the ~10% of WNT pathway-activated medulloblastomas[28] and the *SMARCA4* gene product BRG-1 has been shown to modulate WNT signaling in vascular development, such that BRG-1 loss results in degradation of β-catenin and inhibition of WNT signaling in endothelial cells.[29] The

presence of activating mutations in WNT signaling pathway components in SMARCA4-deficient carcinomas suggests that this subset of sinonasal carcinomas may require WNT pathway activation for tumor initiation or maintenance.

IDH2, and its homolog *IDH1*, are homodimeric enzymes that catalyze the conversion of isocitrate to α-ketoglutarate,[30] and recurrent *IDH1/2* mutations have been identified in a number of solid tumors including gliomas,[31] chondrosarcoma,[32] cholangiocarcinoma,[33] and subsets of AML and angioimmunoblastic T-cell lymphomas.[34,35] These mutations occur almost exclusively at R132 in *IDH1* or in 1 of 2 arginine residues in *IDH2* (R140 or R172). All of these mutations are located in the active site of their respective protein and have been shown to impart a novel function to the protein by which α-ketoglutarate is converted to 2-hydroxyglutarate (2-HG).[30] Under normal conditions, 2-HG has no known function in cells. Recent studies have shown that the accumulation of 2-HG in *IDH*-mutant tumors can act as an α-ketoglutarate antagonist inhibiting several α-ketoglutarate dependent dioxygenases including those involved in DNA and histone demethylation and the TET family of DNA hydroxylases. Inhibition of these enzymes leads to a hypermethylated phenotype that is thought to inhibit cellular differentiation.[36] As neomorphic mutations in *IDH1* and *IDH2* impart a novel function to the enzyme, several drug companies have attempted to develop mutant IDH specific inhibitors that have shown promise in preclinical animal models of AML[16] and glioma.[17] The identification of *IDH* mutations in a substantial subset of SNUC/PDCAR of the sinonasal tract opens new avenues of potential therapy including the IDH2-specific inhibitor AG-221, which has shown promising results in clinical trials[37] and recently received FDA approval for the treatment of *IDH2* mutant relapsed/refractory AML. Other potential therapies include hypomethylating agents, such as 5-azacytidine or decitabine[38,39] or more recently developed PARP inhibitors which have been shown to be effective in *IDH1/2* mutant cells.[40] Using these therapies in conjunction with additional targeted inhibitors (such as to KIT or the PI3K pathway) or conventional chemotherapy may have significant implications for patient management and highlight the utility of genetically characterizing these neoplasms.

In conclusion, *IDH* mutations characterize a molecularly distinct subset of carcinomas within morphologically defined SNUCs, comprising at least one third of this group of tumors in this diagnosis of exclusion. Whether "*IDH*-mutant sinonasal carcinomas" represent a distinct clinicopathologic entity is yet to be determined, but tumors can be identified by a combination of mIDH1/2 IHC and sequencing. While most *IDH*-mutant tumors showed nested growth of uniform epithelioid cells with large vesicular nuclei and prominent nucleoli, *IDH* mutations were also detected in a small number of PDCARs that showed some morphologic features of glandular or neuroendocrine differentiation, which is similar to the findings of Dogan et al[15] and suggests that the presence of an *IDH* mutation can reclassify a subset of PDCAR. However, the morphologic features of *IDH*-mutant sinonasal carcinomas show overlap with many sinonasal malignancies, necessitating a broad IHC panel in which mIDH1/2 IHC may have high diagnostic utility, after exclusion of histologic mimics. We found that both positive and weak mIDH1/2 immunostaining is correlated with the presence of *IDH* mutations, but does not detect all mutations, including *IDH1 R132C* and *IDH2* R172T. While positive mIDH1/2 immunoreactivity may serve as a surrogate marker for the presence of *IDH2* R172 mutations, molecular testing is still necessary for IHC-negative cases. Some cases may show weak mIDH1/2 staining, which likely require molecular confirmation as well. *IDH* mutations can potentially be targeted by mutant IDH inhibitors, therefore accurate identification of *IDH*-mutant sinonasal carcinoma may have significant therapeutic implications.

REFERENCES

1. Llorente JL, Lopez F, Suarez C, et al. Sinonasal carcinoma: clinical, pathological, genetic and therapeutic advances. *Nat Rev Clin Oncol*. 2014;11:460–472.
2. Frierson HF Jr, Mills SE, Fechner RE, et al. Sinonasal undifferentiated carcinoma. An aggressive neoplasm derived from schneiderian epithelium and distinct from olfactory neuroblastoma. *Am J Surg Pathol*. 1986;10:771–779.
3. Reiersen DA, Pahilan ME, Devaiah AK. Meta-analysis of treatment outcomes for sinonasal undifferentiated carcinoma. *Otolaryngol Head Neck Surg*. 2012;147:7–14.
4. Chambers KJ, Lehmann AE, Remenschneider A, et al. Incidence and survival patterns of sinonasal undifferentiated carcinoma in the United States. *J Neurol Surg B Skull Base*. 2015;76:94–100.
5. Lewis JS, Bishop JA, Gillison M, et al. Sinonasal undifferentiated carcinoma. In: El-Naggar AK, Chan JKC, Grandis JR, Takata T, Slootweg PJ, eds. *WHO Classification of Head and Neck Tumours*. Lyon, France: International Agency for Research on Cancer; 2017:18–20.
6. Singh L, Ranjan R, Arava S, et al. Role of p40 and cytokeratin 5/6 in the differential diagnosis of sinonasal undifferentiated carcinoma. *Ann Diagn Pathol*. 2014;18:261–265.
7. French CA, Miyoshi I, Kubonishi I, et al. BRD4-NUT fusion oncogene: a novel mechanism in aggressive carcinoma. *Cancer Res*. 2003;63:304–307.
8. Stelow EB, Bellizzi AM, Taneja K, et al. NUT rearrangement in undifferentiated carcinomas of the upper aerodigestive tract. *Am J Surg Pathol*. 2008;32:828–834.
9. Bishop JA, Guo TW, Smith DF, et al. Human papillomavirus-related carcinomas of the sinonasal tract. *Am J Surg Pathol*. 2013;37:185–192.
10. Bishop JA, Andreasen S, Hang JF, et al. HPV-related multiphenotypic sinonasal carcinoma: an expanded series of 49 cases of the tumor formerly known as HPV-related carcinoma with adenoid cystic carcinoma-like features. *Am J Surg Pathol*. 2017;41:1690–1701.
11. Agaimy A, Hartmann A, Antonescu CR, et al. SMARCB1 (INI-1)-deficient sinonasal carcinoma: a series of 39 cases expanding the morphologic and clinicopathologic spectrum of a recently described entity. *Am J Surg Pathol*. 2017;41:458–471.
12. Bishop JA, Antonescu CR, Westra WH. SMARCB1 (INI-1)-deficient carcinomas of the sinonasal tract. *Am J Surg Pathol*. 2014;38:1282–1289.
13. Agaimy A, Weichert W. SMARCA4-deficient Sinonasal Carcinoma. *Head Neck Pathol*. 2017;11:541–545.
14. Jo VY, Chau NG, Hornick JL, et al. Recurrent IDH2 R172X mutations in sinonasal undifferentiated carcinoma. *Mod Pathol*. 2017;30:650–659.
15. Dogan S, Chute DJ, Xu B, et al. Frequent IDH2 R172 mutations in undifferentiated and poorly-differentiated sinonasal carcinomas. *J Pathol*. 2017;242:400–408.
16. Yen K, Travins J, Wang F, et al. AG-221, a first-in-class therapy targeting acute myeloid leukemia harboring oncogenic IDH2 mutations. *Cancer Discov*. 2017;7:478–493.
17. Kopinja J, Sevilla RS, Levitan D, et al. A brain penetrant mutant IDH1 inhibitor provides in vivo survival benefit. *Sci Rep*. 2017;7:13853.

18. Sholl LM, Do K, Shivdasani P, et al. Institutional implementation of clinical tumor profiling on an unselected cancer population. *JCI Insight*. 2016;1:e87062.
19. Garcia EP, Minkovsky A, Jia Y, et al. Validation of OncoPanel: a targeted next-generation sequencing assay for the detection of somatic variants in cancer. *Arch Pathol Lab Med*. 2017;141: 751–758.
20. Guo J, Carvajal RD, Dummer R, et al. Efficacy and safety of nilotinib in patients with KIT-mutated metastatic or inoperable melanoma: final results from the global, single-arm, phase II TEAM trial. *Ann Oncol*. 2017;28:1380–1387.
21. Kato Kaneko M, Ogasawara S, Kato Y. Establishment of a multi-specific monoclonal antibody MsMab-1 recognizing both IDH1 and IDH2 mutations. *Tohoku J Exp Med*. 2013;230:103–109.
22. Liu X, Kato Y, Kaneko MK, et al. Isocitrate dehydrogenase 2 mutation is a frequent event in osteosarcoma detected by a multi-specific monoclonal antibody MsMab-1. *Cancer Med*. 2013;2: 803–814.
23. Ali SM, Yao M, Yao J, et al. Comprehensive genomic profiling of different subtypes of nasopharyngeal carcinoma reveals similarities and differences to guide targeted therapy. *Cancer*. 2017;123:3628–3637.
24. Lui VWY, To KF, Lo KW. Genomic profiles of nasopharyngeal carcinoma: the importance of histological subtyping and Epstein-Barr virus in situ assays. *Cancer*. 2018;124:434–435.
25. Li YY, Chung GT, Lui VW, et al. Exome and genome sequencing of nasopharynx cancer identifies NF-kappaB pathway activating mutations. *Nat Commun*. 2017;8:14121.
26. Lin DC, Meng X, Hazawa M, et al. The genomic landscape of nasopharyngeal carcinoma. *Nat Genet*. 2014;46:866–871.
27. Zheng H, Dai W, Cheung AK, et al. Whole-exome sequencing identifies multiple loss-of-function mutations of NF-kappaB pathway regulators in nasopharyngeal carcinoma. *Proc Natl Acad Sci U S A*. 2016;113:11283–11288.
28. Northcott PA, Jones DT, Kool M, et al. Medulloblastomics: the end of the beginning. *Nat Rev Cancer*. 2012;12:818–834.
29. Griffin CT, Curtis CD, Davis RB, et al. The chromatin-remodeling enzyme BRG1 modulates vascular Wnt signaling at two levels. *Proc Natl Acad Sci U S A*. 2011;108:2282–2287.
30. Clark O, Yen K, Mellinghoff IK. Molecular pathways: isocitrate dehydrogenase mutations in cancer. *Clin Cancer Res*. 2016;22:1837–1842.
31. Yan H, Parsons DW, Jin G, et al. IDH1 and IDH2 mutations in gliomas. *N Engl J Med*. 2009;360:765–773.
32. Amary MF, Bacsi K, Maggiani F, et al. IDH1 and IDH2 mutations are frequent events in central chondrosarcoma and central and periosteal chondromas but not in other mesenchymal tumours. *J Pathol*. 2011;224:334–343.
33. Borger DR, Tanabe KK, Fan KC, et al. Frequent mutation of isocitrate dehydrogenase (IDH)1 and IDH2 in cholangiocarcinoma identified through broad-based tumor genotyping. *Oncologist*. 2012;17:72–79.
34. Cairns RA, Iqbal J, Lemonnier F, et al. IDH2 mutations are frequent in angioimmunoblastic T-cell lymphoma. *Blood*. 2012;119:1901–1903.
35. Mardis ER, Ding L, Dooling DJ, et al. Recurring mutations found by sequencing an acute myeloid leukemia genome. *N Engl J Med*. 2009; 361:1058–1066.
36. Dang L, Yen K, Attar EC. IDH mutations in cancer and progress toward development of targeted therapeutics. *Ann Oncol*. 2016;27:599–608.
37. Stein EM, DiNardo CD, Pollyea DA, et al. Enasidenib in mutant IDH2 relapsed or refractory acute myeloid leukemia. *Blood*. 2017; 130:722–731.
38. Borodovsky A, Salmasi V, Turcan S, et al. 5-azacytidine reduces methylation, promotes differentiation and induces tumor regression in a patient-derived IDH1 mutant glioma xenograft. *Oncotarget*. 2013;4:1737–1747.
39. Turcan S, Fabius AW, Borodovsky A, et al. Efficient induction of differentiation and growth inhibition in IDH1 mutant glioma cells by the DNMT inhibitor decitabine. *Oncotarget*. 2013;4:1729–1736.
40. Sulkowski PL, Corso CD, Robinson ND, et al. 2-Hydroxyglutarate produced by neomorphic IDH mutations suppresses homologous recombination and induces PARP inhibitor sensitivity. *Sci Transl Med*. 2017;9.